The Effect of Low Concentrations of Molecularly Dispersed Poly(Vinylpyrrolidone) on Indomethacin Crystallization from the Amorphous State

Kieran J. Crowley [1] and George Zografi [2,3]

Received May 10, 2003; accepted May 23, 2003

Purpose. To investigate the effect of low concentrations of molecularly dispersed poly(vinylpyrrolidone) (PVP) on indomethacin (IMC) crystallization from the amorphous state using particle size effects to identify possible mechanisms of crystallization inhibition.
Methods. Different particle sizes of amorphous IMC and 1, 2, and 5% PVP were stored dry at 30°C for 84 days. PXRD was used to calculate the rate and extent of crystallization and the polymorph formed.
Results. Crystallization from amorphous IMC and IMC/PVP molecular dispersions yielded the γ polymorph of IMC. Crystallization rates were reduced at larger particle size and in the presence of 1, 2, and 5%PVP. Crystallization did not reach completion in some IMC/PVP samples, with the quantity of uncrystallized amorphous phase proportional to particle size.
Conclusions. Low concentrations of molecularly dispersed PVP affected IMC crystallization from the amorphous state. Formation of γ-IMC at rates dependent on particle size indicated that surface nucleation predominated in both the absence and presence of PVP. Excellent correlation was seen between the extent of crystallization and simulated depths of crystal penetration, supporting the hypothesis that increasing local PVP concentration inhibits crystal growth from surface nuclei into the amorphous particle.

KEY WORDS: molecular dispersions; particle size; crystal nucleation; crystal growth.

INTRODUCTION

Extensive characterization of the model pharmaceutical glass-former indomethacin (IMC) has generated important information regarding the relationship among molecular mobility, intermolecular interactions, and the physical stability of the amorphous state (1–7). Imaizumi *et al.* demonstrated that isothermal crystallization of quenched amorphous IMC took place both above and immediately below the glass transition temperature (T_g) (1). Isothermal crystallization below T_g produced the stable γ polymorph, whereas isothermal crystallization above T_g proceeded at much faster rates to form principally the metastable α polymorph (1,3,8). With a T_g of approximately 40°C, amorphous IMC is physically unstable at room temperature over long time periods.

The physical stability of amorphous IMC at room temperature can be markedly improved by forming a molecular dispersion with poly(vinylpyrrolidone) (PVP) (9,10). Concentrations of 10% PVP (by weight) and above increase the T_g of amorphous IMC and thus would be expected to improve amorphous state stability via an antiplasticizing effect. Matsumoto and Zografi, however, found that an IMC/PVP molecular dispersion containing 5% PVP (by weight) remained physically stable for at least 140 days at 30°C, even though this PVP concentration had only a minor effect on T_g (11). This finding suggests an additional inhibitory effect of PVP on amorphous IMC crystallization. Although the exact mechanism has not been elucidated, solid-state vibrational spectroscopy demonstrated that PVP hydrogen bonds with IMC in molecular dispersions (6) and disrupts the formation of IMC dimers, which appear critical for crystal nucleation.

The aim of this study was to examine more closely the crystallization behavior of amorphous IMC in the presence of low concentrations of molecularly dispersed PVP (1, 2, and 5% by weight) with the following objectives: (a) to establish if there is a lower concentration limit governing the effect of PVP on amorphous IMC crystallization and (b) to identify the likely mechanism of IMC crystallization inhibition by PVP at low PVP concentrations. Four different particle size fractions of each amorphous system were examined because any relationship between particle size and crystallization behavior could provide additional insight into the mechanisms of IMC crystal nucleation and growth in the amorphous state, and how these processes may be affected by molecularly dispersed PVP.

MATERIALS

The chemical structures of IMC and PVP monomer are shown in Fig. 1. γ-IMC (Sigma, St. Louis, MO) was converted to the amorphous form by heating at 180°C for approximately 5 min, followed by quench cooling to room temperature. Poly(vinylpyrrolidone) K90 (BASF, Ludwigshafen, Germany) was dried at 120°C for 12 h before use. A two-step process was used to prepare IMC/PVP dispersions in the concentration range 1 to 5% PVP (all units expressed as weight percent). First, a 10% PVP molecular dispersion was prepared by rota-evaporation from methanol as described previously (10) and dried at 40°C for 24 h. Rota-evaporation could not be used to prepare the 1 and 2% PVP dispersions because partial IMC crystallization would occur during preparation. Instead, the 10% PVP dispersion was diluted with pure amorphous IMC to yield physical mixtures containing 1, 2, and 5% PVP. On a 5-g scale, physical mixtures were heated at 180°C for approximately 5 min (with intermittent stirring to aid mixing of the molten sample) and then allowed to cool to room temperature to yield quenched cooled molecular dispersions of 1, 2, and 5% PVP composition. In a dry N_2 glove bag, quenched cooled IMC and PVP dispersions were lightly ground, and the following particle size ranges were isolated using 3″ diameter stainless steel sieves (W. S.Tyler, Mentor, OH): 0–40 μm (#1), 75–150 μm (#2), 250–425 μm (#3), and 610–700 μm (#4). The 5% PVP size #4 was not studied because of a low yield of this size fraction. Specific surface areas of IMC particle size samples were measured using krypton adsorption and BET analysis with a model 1M0325 Quantasorb Surface Area Analyzer (Quantachrome, Syosset, NY). Values for four samples were 0.628 m^2/g (#1), 0.120 m^2/g (#2), 0.044 m^2/g (#3), and 0.024 m^2/g (#4).

[1] AnorMED Inc., Langley, British Columbia V2Y 1N5, Canada.
[2] School of Pharmacy, University of Wisconsin-Madison, Madison, Wisconsin 53705.
[3] To whom correspondence should be addressed. (email: gdzografi@pharmacy.wisc.edu)

0724-8741/03/0900-1417/0 © 2003 Plenum Publishing Corporation

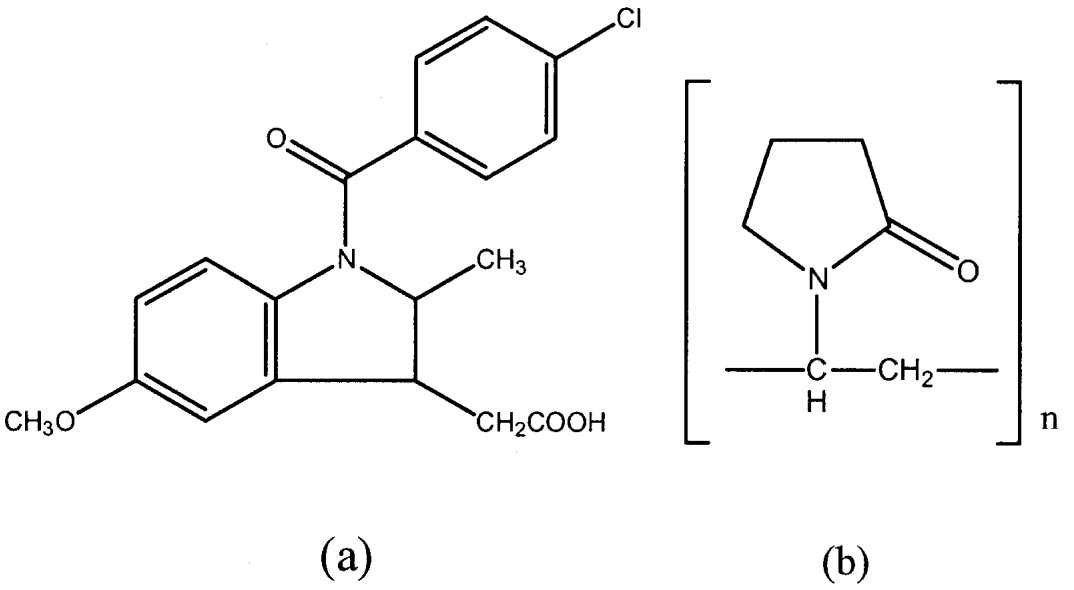

Fig. 1. Chemical structures of (a) IMC and (b) a PVP monomer unit.

METHODS

Powder X-Ray Diffraction

Isothermal crystallization studies were performed in 2-mm i.d. glass capillaries stored in a glass jar containing desiccant at 30°C. Powder X-ray diffraction (PXRD) was performed using the General Area Detector Diffraction System (Siemens, Madison, WI) with CuK_α radiation generated at 40 kV and 20 mA. Diffraction patterns were measured *in situ* by rotating glass capillaries containing sample within the X-ray beam without the need for sample grinding or trituration. Following background subtraction, the peak height at 11.8°2θ was used to quantify γ IMC, using physical mixtures of amorphous and crystalline γ IMC to generate a standard curve, as previously reported (12). Duplicate PXRD measurements were made for each data point. For samples that underwent complete crystallization, a crystallization rate constant k was calculated based on the KJMA equation (13):

$$x = 1 - \exp(-(k(t - t_0))^n) \quad (1)$$

where x is the weight fraction crystallized after time t and an experimental induction time t_o. With an exponent n of 1, the linear form of this equation was used to calculate k by linear regression with R^2 coefficients of determination given with each data set.

Differential Scanning Calorimetry

The Seiko SSC220C DSC instrument (Haake, Paramus, NJ) was used to perform differential scanning calorimetry (DSC) at a heating rate of 2°C/min and a 100 ml/min N_2 purge. Aluminum pans with lids were used without crimping to prevent crushing the sample so as to retain the original particle size. Temperature and enthalpy calibration were performed using indium and gallium (Aldrich, Milwaukee, WI). Glass transition temperature (T_g) was calculated using the extrapolated onset temperature.

RESULTS

Isothermal Crystallization of IMC

PXRD data recording the isothermal crystallization of IMC #1 at 30°C are shown in Fig. 2a. The diffraction patterns indicated the formation of γ-IMC in agreement with previously reported data for quenched amorphous IMC (12). Isothermal crystallization of IMC sizes #2 to #4 also produced the γ polymorph only. Plots of percentage crystallinity vs. time for IMC particle sizes #1 to #4 (Fig. 3a) show that the rate of γ-IMC crystallization decreased with increased particle size. All IMC samples #1 to #4 underwent complete crystallization during the experimental time scale, a finding confirmed by the absence of a T_g or crystallization event in DSC data for samples measured at the final time point (data not shown). Crystallization rate constants of 0.285, 0.149, 0.0659, and 0.0375 day^{-1} were calculated for IMC particle sizes #1, #2, #3, and #4, respectively (see Table I).

Isothermal Crystallization of IMC from IMC/PVP Molecular Dispersions

Four particle sizes of 1% PVP (#1–4) and 2% PVP (#1–4) and three sizes of 5% PVP (#1–3) were characterized by PXRD during storage at 30°C for 84 days. Raw PXRD data for size #1 samples in Fig. 2b–d showed crystallization of the γ polymorph in the presence of 1, 2, and 5% PVP. Formation of exclusively γ-IMC was demonstrated at all PVP concentrations and all sizes with the exception of 5% PVP size #3, for which no crystallization was detected. Plots of percentage crystallinity vs. time for 1, 2, and 5% PVP dispersions are shown in Fig. 3b–d. Size #1 samples of 1% and 2% PVP approached complete crystallization during the experimental time period so kinetic analysis using the KJMA equation was restricted to these samples only. At a single particle size, increasing PVP dispersion concentration from 0% PVP to 1% PVP and 2% PVP caused a reduction in k from 0.285 day^{-1} to 0.103 day^{-1} and 0.0325 day^{-1} (Table II). Although crystalli-

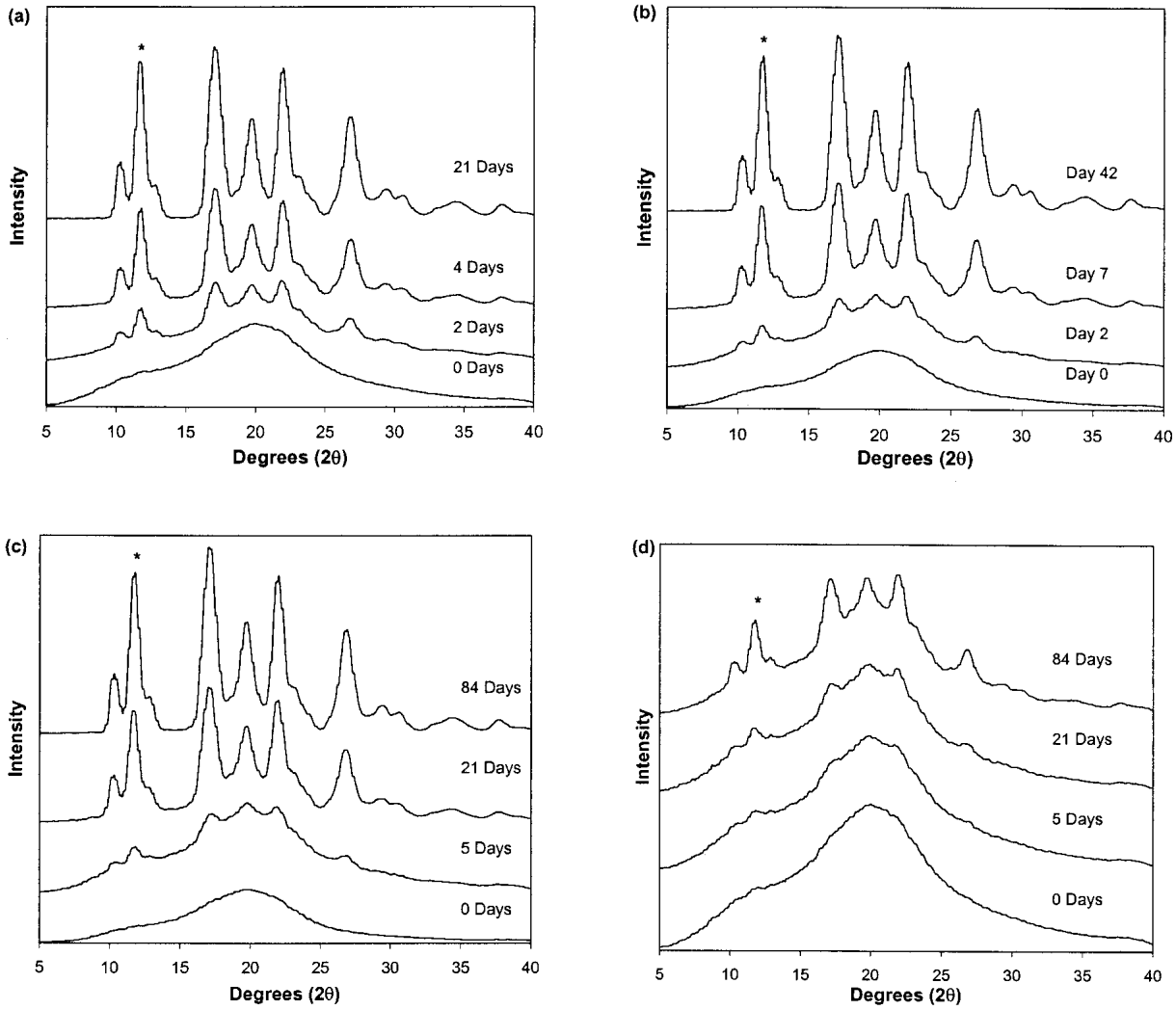

Fig. 2. PXRD data recording crystallization of γ-IMC at 30°C from (a) amorphous IMC, (b) 1% PVP dispersion, (c) 2% PVP dispersion, (d) 5% PVP dispersion. The symbol * marks the diffraction peak used for γ IMC quantification.

zation rate constants were not calculated for larger-particle-size PVP samples, the amount of crystal phase forming at the earliest time points was seen to reduce with increasing PVP concentration. At a single PVP concentration, increasing particle size caused reduction in the initial levels of crystal phase. Larger particle sizes of 1% and 2% PVP samples exhibited rapid changes in crystallinity at early time points (between 0 and 30–40 days) followed by a fall in crystallization rate at later time points. The reduction in crystallization rate after 30-40 days was so marked that the degree of crystallinity underwent only a small change in the remaining time period and so appeared to approach a plateau level of crystallinity. PXRD measurements were not made beyond 84 days, so it was not possible to confirm whether crystallization ceased to leave a partially crystalline sample or if crystallization would have continued at an extremely slow rate until all amorphous phase had crystallized. The extent of crystallization, i.e., the crystal phase concentration in the plateau region, decreased with increasing particle size.

Glass transition temperatures for all particle sizes of IMC and PVP dispersions ranged from 38 to 44°C (see Table III). T_g was constant for the four particle sizes of 2% PVP and remained within a range of 3°C or lower for IMC, 1% PVP, and 5% PVP samples, indicating that particle size did not have a large effect on T_g. Average T_g values for IMC, 1%, 2%, and 5% PVP were 43, 41, 44, and 39°C, respectively, so there is no relationship between PVP concentration and T_g. Such scatter among average T_g values could have been due to differences in enthalpic relaxation at the glass transition that affected the integration of T_g. Exothermic transitions were seen on DSC analysis of IMC and IMC/PVP samples. These data were indicative of crystallization events accompanied by polymorphic transitions as seen previously with IMC (12). Because of the poor resolution of the exothermic events for some samples, it was not possible to identify a nonisothermal crystallization temperature or enthalpy for all samples, so a correlation between particle size and crystallization tendency could not be identified.

DISCUSSION

This study demonstrates that 1 to 5% molecularly dispersed PVP reduces the rate of IMC crystallization below T_g relative to equivalent particle size fractions of quenched

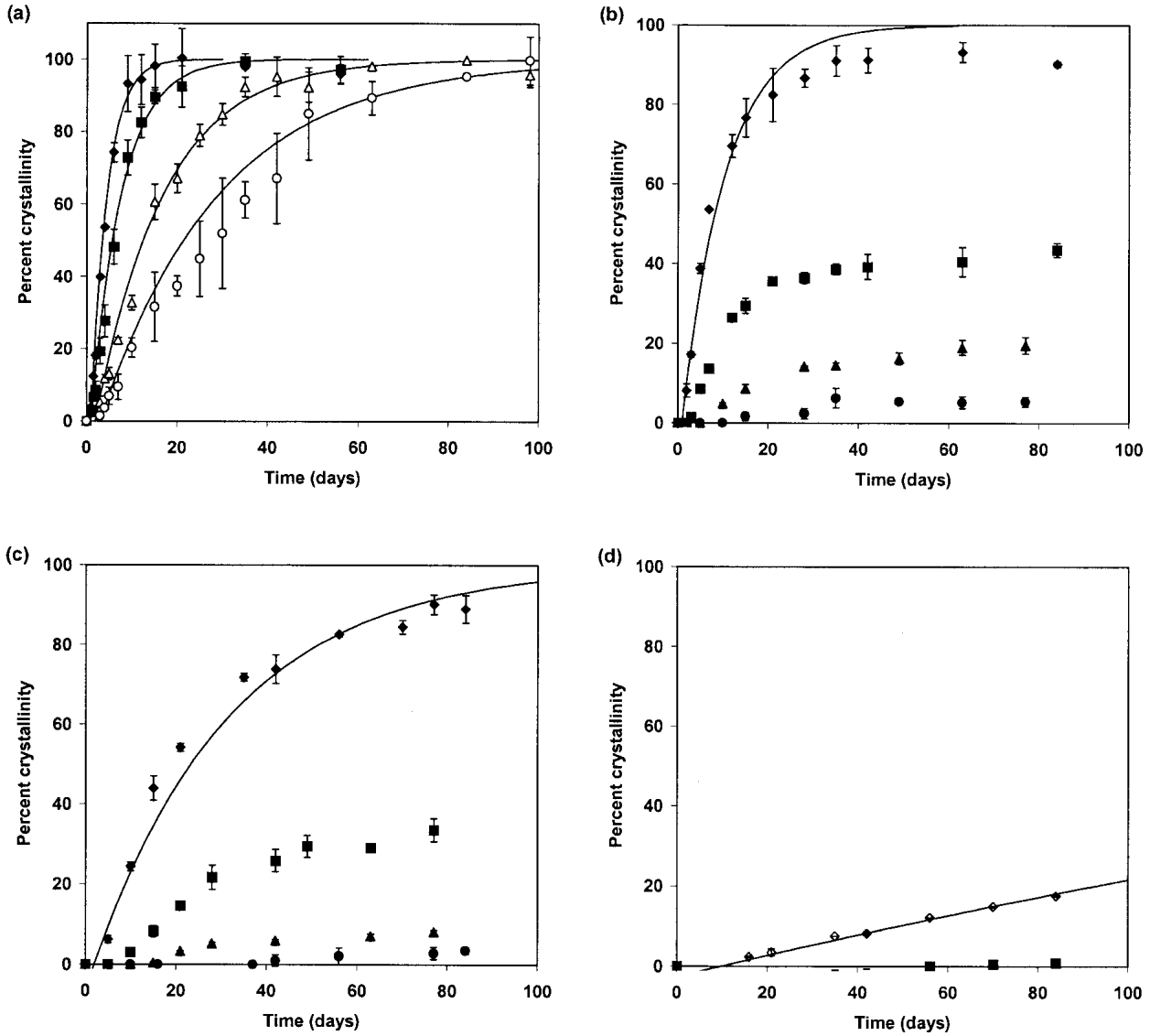

Fig. 3. Percentage crystal phase against time plots for different particle sizes of (a) amorphous IMC, (b) 1% PVP dispersion, (c) 2% PVP dispersion, (d) 5% PVP dispersion. Errors bars represent the range for duplicate measurements. The legend for particle sizes is ♦(#1), ■ (#2), ▲(#3), ● (#4) and the solid lines represent a best fit to the KJMA equation.

amorphous IMC. These findings add to an earlier report showing that 5% dispersed PVP completely inhibits crystallization of IMC at 30°C for 140 days (11). Data from the two studies compare favorably, since Matsumoto and Zografi (11) used a particle size less than 200 μm, which corresponded to between sizes #2 and #3 in the current study. The negligible antiplasticizing effect of 5% PVP on amorphous IMC reported in previous work was confirmed in the current work as T_g values for IMC and 1 to 5% PVP dispersions are comparable.

Throughout this discussion, it is assumed that the different amorphous particle size fractions of each PVP dispersion possess the same chemical composition and bulk properties, notably amorphous phase structure and energetics. These assumptions are supported by the low variation in T_g measured

Table I. KJMA Isothermal Crystallization Parameters for Sizes #1 to #4 of Amorphous IMC

Amorphous IMC sample	t_o [days]	k [day^{-1}]	KJMA R^2
#1 (<40 μm)	0	0.285	0.983
#2 (75–150 μm)	0	0.149	0.990
#3 (250–425 μm)	0	0.0659	0.969
#4 (600–710 μm)	0	0.0375	0.976

Table II. KJMA Analysis of Isothermal Crystallization of Size #1 Amorphous IMC, 1%, 2%, and 5% PVP Dispersions at 30°C

Sample	t_o [days]	k [day^{-1}]	KJMA R^2
Amorphous IMC #1	0	0.285	0.983
1% PVP dispersion #1	1	0.103	0.985
2% PVP dispersion #1	2	0.0325	0.977

Table III. The Glass Transition Temperature for Particle Sizes #1 to #4 of Amorphous IMC and 1, 2, and 5% PVP Dispersions

Sample	IMC	1% PVP	2% PVP	5% PVP
#1 (<40 μm)	42°C	43°C	44°C	38°C
#2 (75–150 μm)	43°C	40°C	44°C	40°C
#3 (250–425 μm)	43°C	40°C	44°C	38°C
#4 (600–710 μm)	42°C	41°C	44°C	—
Average	43°C	41°C	44°C	39°C

by DSC analysis for the different particle sizes of 1, 2, and 5% PVP. An additional consideration is that the different size fractions isolated by grinding and sieving may possess different surface properties such as roughness, energetics, or particulate contamination, each of which could affect nucleation phenomena.

The relationship between particle size and crystallization rate of pure amorphous IMC has been described previously and is a result of this system undergoing surface nucleation (8,14). The fact that the particle size effect on IMC crystallization rate is retained in the presence of 1 to 5% PVP, and that the polymorph formed does not change, suggests that the mechanism of crystal nucleation is unchanged. Kinetic analysis of crystallization using the KJMA equation can yield information on the mechanisms of crystal nucleation and growth in solution, with an n value of 4 predicted for a system undergoing continuous nucleation and an n of 3 predicted for growth from a fixed number of nuclei. When crystallization is examined from the amorphous state below T_g, however, n values much lower than 3 to 4 are commonly obtained, the cause of which may be nonrandom nucleation or relaxation of the amorphous phase as crystallization proceeds (15). In this study, an n of 1 gives the best R^2 coefficient of determination values (>0.969). It is not thought that the magnitude of n reveals information related to crystallization mechanisms for the current data sets, so it is used solely for calculating crystallization rate constants. IMC k decreases by a factor of approximately 2 with each successive increase in particle size and decreases by a factor of approximately 3 on introduction of 1% increments of molecularly dispersed PVP (based on size #1 data only).

The large effect of particle size on the extent of crystallization at all PVP concentrations provides evidence of an effect of molecularly dispersed PVP on IMC crystal growth. At 1% PVP, the proportion of IMC crystallized in sizes #1 to #4 changes from 90% to less than 10% at the first time point. The time taken for crystal phase to reach the plateau region remains in the range of 30 to 40 days for all particle sizes. A possible explanation of this behavior is that relaxation of the amorphous phase during crystallization reduces molecular mobility such that crystal growth slows or ceases. This theory can be discounted because pure amorphous IMC underwent complete crystallization over an 84-day period despite the fact that substantial relaxation will have occurred during this time period.

An alternative explanation for incomplete IMC crystallization in the presence of PVP is that the local PVP concentration in the amorphous phase changes as IMC crystallization proceeds. Assuming that polymer is not incorporated into the IMC crystal, PVP must remain either in the amorphous phase or at the amorphous–crystalline interface. Both scenarios would lead to increases in local polymer concentration that could restrict further crystal growth into the amorphous bulk. Following surface nucleation, crystal growth would penetrate the amorphous bulk at the same rate in all particle sizes until a critical local concentration of PVP is reached. The degree of crystal phase penetration into amorphous bulk will be constant at different particle sizes, but the quantity of uncrystallized amorphous phase will change. This hypothesis can explain why the time taken to reach a plateau of crystallized phase in different particle sizes of 1% PVP is constant, but the amount of crystallized phase varied widely.

To test this hypothesis, we can simulate how a constant depth of crystal phase penetration into amorphous bulk will affect the total quantity of crystal phase in a spherical particle. Almost complete crystallization takes place in the 1% PVP size #1 particles, so this particle size provides an approximation of the minimum depth of crystal penetration. If particles in this size range (0–40 μm) are spherical with an average diameter of 20 μm, crystallization will occur to a depth of 10 μm perpendicular to the surface. Calculation of the volume of crystallized phase in spherical particles at the larger particle sizes #2, #3, and #4 (average particle diameters 112.5, 335.5, and 655 μm) yields percentage crystallinity values of 44, 17, and 9%, respectively (see Table IV). These values are very consistent with the experimental plateau crystallinity levels of 43, 21, and 6% measured for sizes #2, #3, and #4 after approximately 84 days.

The same procedure is now used to predict plateau crystallinity of 2%PVP samples sizes #2, #3 and #4. We assume that doubling of starting PVP concentration will reduce the depth of crystal growth into the bulk from 10 to 5 μm for this simulation. Crystallization to a depth of 5 μm into a size #1 spherical particle with 10 μm radius would produce 88% crystal phase by volume. The experimental crystallinity value for 2% PVP size #1 at 84 days was 89% so the model appears to be suitable at the higher PVP concentration also. Predicted percent crystal phase values at the plateau region are 24%, 9% and 5% for sizes #2, #3 and #4, again showing good agreement with experimental crystallinity after approximately 84 days of 33%, 8% and 4%, respectively. The assumptions of the presence of spherical particles possessing a single particle

Table IV. Predicted and Experimental Levels of Crystal Content of 1% PVP and 2% PVP Dispersions following Approximately 84 Days of Storage at 30°C[a]

Sample	Predicted crystal content	Experimental crystal content
1%PVP dispersion		
#1	100%	90%
#2	44%	43%
#3	17%	21%
#4	9%	6%
2%PVP dispersion		
#1	88%	89%
#2	24%	33%
#3	9%	8%
#4	5%	4%

[a] Predictions were made assuming constant depth of crystal penetration into spherical particles with diameter of the sieve size fraction midpoint.

size at the midpoint of the sieve size fraction and of a constant depth of crystallization into such particles are clearly a simplification of the real system. We recognize that the shape and size distribution of a true sample will be irregular and dispersed and that the extent of crystal growth into the solid amorphous phase will vary according to heterogeneities in the starting amorphous phase and as a result of physical changes taking place as crystallization proceeds. Nevertheless, the remarkable agreement between predicted and experimental plateau region crystallinity means that the proposal of local PVP concentration contributing to inhibition of IMC crystal growth below T_g is plausible. Mechanisms of crystal growth inhibition by PVP could be a local antiplasticization effect, a change in the crystal–amorphous interfacial energy, or the hydrogen-bonding interaction between IMC and PVP, as demonstrated previously (6).

CONCLUSIONS

The rate of IMC crystallization in IMC/PVP molecular dispersions stored isothermally below T_g was reduced relative to pure amorphous IMC in the concentration range 1 to 5% PVP. Formation of the γ-IMC polymorph in 1 to 5% PVP molecular dispersions suggested that the mechanism of nucleation was unaffected by low levels of PVP. This conclusion was supported by the finding that particle size had a large effect on crystallization rates in both amorphous IMC and 1 to 5% PVP, indicating surface-mediated nucleation in all samples.

All particle sizes of pure amorphous IMC underwent complete crystallization over 84 days of storage at 30°C. Larger particle sizes of 1% and 2% PVP molecular dispersions partially crystallized at early time points but reached a constant level of crystal and amorphous phase that remained stable for the remainder of the study. The plateau region of crystallinity was dependent on particle size, but the time taken to reach steady state was independent of particle size. These data were explained by an increasing local PVP concentration in close proximity to the crystallized phase that reached a critical level to inhibit crystal growth further into the bulk of amorphous particles.

ACKNOWLEDGMENTS

We wish to acknowledge The Purdue-Wisconsin Program on the Physical and Chemical Stability of Pharmaceutical Solids for generous financial support, and Professor Juan DePablo and colleagues in the Department of Chemical Engineering, UW-Madison, for access to PXRD equipment.

REFERENCES

1. H. Imaizumi, N. Nambu, and T. Nagai. Stability and several physical properties of amorphous and crystalline forms of indomethacin. *Chem. Pharm. Bull.* **28**:2565–2569 (1980).
2. E. Fukuoka, M. Makita, and S. Yamamura. Some physicochemical properties of glassy indomethacin. *Chem. Pharm. Bull.* **34**: 4314–4321 (1986).
3. M. Yoshioka, B. Hancock, and G. Zografi. Crystallization of indomethacin from the amorphous state below and above its glass transition temperature. *J. Pharm. Sci.* **83**:1700–1705 (1994).
4. B. C. Hancock, S. L. Shamblin, and G. Zografi. Molecular mobility of amorphous pharmaceutical solids below their glass transition temperatures. *Pharm. Res.* **12**:799–806 (1995).
5. V. Andronis and G. Zografi. Molecular mobility of supercooled amorphous indomethacin determined by dynamic mechanical analysis. *Pharm. Res.* **14**:410–414 (1997).
6. L. S. Taylor and G. Zografi. Spectroscopic characterization of interactions between PVP and indomethacin in amorphous molecular dispersions. *Pharm. Res.* **14**:1691–1698 (1997).
7. V. Andronis and G. Zografi. The molecular mobility of supercooled amorphous indomethacin as a function of temperature and relative humidity. *Pharm. Res.* **15**:835–842 (1998).
8. V. Andronis, M. Yoshioka, and G. Zografi. Effects of sorbed water on the crystallization of indomethacin from the amorphous state. *J. Pharm. Sci.* **86**:346–350 (1997).
9. H. Imaizumi, N. Nambu, and T. Nagai. Stabilization of amorphous state of indomethacin by solid dispersion in polyvinylpyrrolidone. *Chem. Pharm. Bull.* **31**:2510–2512 (1983).
10. M. Yoshioka, B. C. Hancock, and G. Zografi. Inhibition of indomethacin crystallization in poly(vinylpyrrolidone) coprecipitates. *J. Pharm. Sci.* **84**:983–986 (1995).
11. T. Matsumoto and G. Zografi. Physical properties of solid molecular dispersion of indomethacin with poly(vinylpyrrolidone) and poly(vinylpyrrolidone-co-vinyl-acetate) in relation to indomethacin crystallization. *Pharm. Res.* **16**:2376–2380 (1999).
12. K. J. Crowley and G. Zografi. Cryogenic grinding of indomethacin polymorphs and solvates: assessment of amorphous phase formation and amorphous phase physical stability. *J. Pharm. Sci.* **91**:492–502 (2002).
13. J. W. Mullin. *Crystallization*, Butterworths, Oxford, UK, 1993.
14. V. Andronis and G. Zografi. Crystal nucleation and growth of indomethacin polymorphs from the amorphous state. *J. Non Cryst. Solids* **271**:236–248 (2000).
15. C. W. Price. Use of Kolmogorov-Johnson-Mehl-Avrami kinetics in recrystallization of metals and crystallization of metallic glasses. *Acta Metall. Mater.* **38**:727–738 (1990).